

Dispersible Ferromagnetic FePt Nanoparticles

By Jaemin Kim, Chuanbing Rong, J. Ping Liu, and Shouheng Sun*

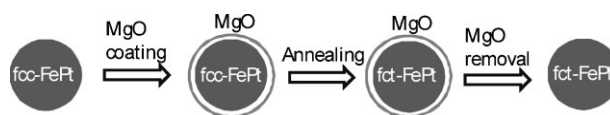
The synthesis of ferromagnetic (FM) FePt nanoparticles (NPs) has attracted much attention in magnetic NP research.^[1] Such NPs, with controlled magnetic properties, have great potential for ultrahigh-density information-storage^[2–4] and high-performance permanent-magnet applications.^[5–9] Monodisperse FePt NPs have been produced by solution-phase chemical decomposition of iron pentacarbonyl ($\text{Fe}(\text{CO})_5$) and reduction of platinum acetylacetonate ($\text{Pt}(\text{acac})_2$),^[10–13] or by co-reduction of an iron and a platinum salt.^[14–19] As synthesized, the FePt NPs have a chemically disordered face-centered cubic (fcc) structure, and are superparamagnetic at room temperature. FM FePt NPs with a face-centered tetragonal (fct) structure can only be obtained by thermal annealing of fcc-FePt NPs at high temperatures (usually higher than 550 °C). This high-temperature annealing renders FM FePt NPs undispersible, and unsuitable for controlled assembly and for single-particle magnetism studies. To make dispersible FM FePt NPs, one can coat the as-synthesized FePt NPs with SiO_2 before thermal annealing, and remove SiO_2 after the fct FePt is formed.^[20–23] Alternatively, the as-synthesized FePt NPs can be ground with a large excess of NaCl before thermal annealing – the fine grains of NaCl protect the FePt NPs from sintering at high-temperature-annealing conditions, and NaCl can be dissolved with water.^[24–27] Despite these efforts, stabilizing a FM FePt-NP dispersion is still challenging.

Here, we report a new synthesis and stabilization strategy, as outlined in Scheme 1, to produce a FM FePt-NP dispersion in a hydrocarbon solvent. During the preparation, we first coat the as-synthesized fcc-FePt NPs with MgO – a basic oxide that is thermally stable, with a melting point of 2000 °C, and that can react with HCl to form MgCl_2 and water. MgO protects the fcc-FePt NPs from aggregation at annealing temperatures up to 800 °C, and the fcc FePt is converted to fct FePt at above 700 °C. Dissolving MgO with 0.5 M HCl in the presence of a hexane solution of hexadecanethiol (HDT) and oleic acid (OA) leads to well-dispersed FM fct-FePt NPs in hexane. The fct-FePt NPs show coercivity up to 1 T at room temperature, and a magnetization of 56.4 emu per gram of FePt.

The 7 nm fcc- $\text{Fe}_{51}\text{Pt}_{49}$ NPs were synthesized according to a previously published method.^[12] During the synthesis, 0.5 mmol of $\text{Pt}(\text{acac})_2$, 4 mmol of OA, 4 mmol of oleylamine (OAm), and 10 mL of octadec-1-ene were mixed with 0.20 mL of $\text{Fe}(\text{CO})_5$ and heated to 240 °C for 1 h. Figure 1a and 1b shows the transmission

electron microscopy (TEM) images of two-dimensional assemblies of the monodisperse 7 nm fcc-FePt NPs. While the monolayer assembly in Figure 1a illustrates a typical hexagonal close packing, the double-layer assembly in Figure 1b shows an anomalous array, where the second layer sits on the two-fold saddle points. This is similar to what is reported for Au NP assemblies.^[28] MgO was coated on the $\text{Fe}_{51}\text{Pt}_{49}$ NPs by decomposition of $\text{Mg}(\text{acac})_2$ in the presence of tetradecane-1,2-diol, OA, and OAm in benzyl ether, and heated to 298 °C. Figure 1c is the TEM image of the 7 nm $\text{Fe}_{51}\text{Pt}_{49}/\text{MgO}$ NPs with a MgO coating over the FePt surface.

Thermal annealing of the fcc-FePt/MgO and fcc-FePt NPs was performed under Ar + 5% H_2 at various temperatures. For the fcc-FePt/MgO NP assemblies, TEM analyses indicated that for annealing below 800 °C for less than 4 h, there was no obvious FePt morphology change in the FePt/MgO structure, and MgO formed a flower-like pattern, as shown in Figure 1d. However,



Scheme 1. Synthesis of fct-FePt NPs from fcc-FePt/MgO NPs.

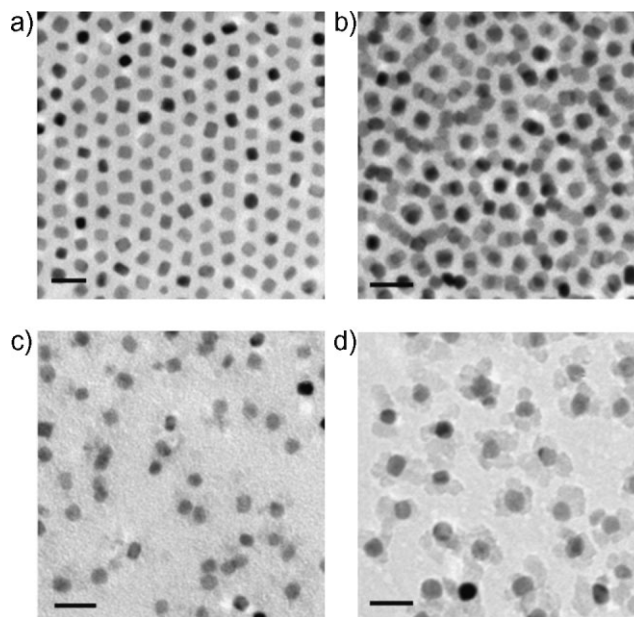


Figure 1. TEM images of a) 7 nm fcc-FePt NPs, b) abnormal assembly of the 7 nm fcc-FePt, c) as-synthesized fcc-FePt/MgO NPs, and d) fct-FePt/MgO NPs obtained from thermal annealing of the fcc-FePt/MgO NPs under Ar + 5% H_2 at 750 °C for 6 h. Scale bar = 20 nm.

[*] Prof. S. Sun, J. Kim
Department of Chemistry, Brown University
Providence, Rhode Island 02912 (USA)
E-mail: ssun@brown.edu

Dr. C. Rong, Prof. J. P. Liu
Department of Physics
University of Texas at Arlington
Arlington, Texas 76019 (USA)

DOI: 10.1002/adma.200801620

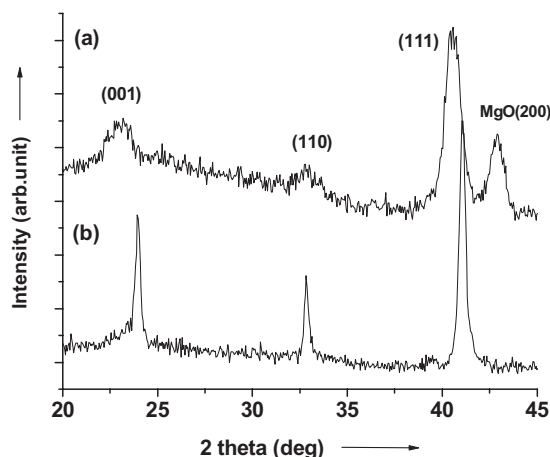


Figure 2. XRD patterns of a) fct-FePt/MgO NP and b) fct-FePt NP assemblies obtained from the thermal annealing of the fcc-FePt/MgO and the fcc-FePt NP assemblies at 750 °C for 6 h in the Ar + 5% H₂ atmosphere.

upon annealing at 800 °C for over 6 h, these FePt/MgO NPs sintered. X-ray diffraction (XRD) analyses of the annealed FePt/MgO assemblies revealed that an fcc-to-fct structure transformation in the FePt NPs is not readily characterized until the annealing temperature reaches above 700 °C. Figure 2a is the XRD pattern of the fct-FePt/MgO assembly obtained from the annealing of the fcc-FePt/MgO at 750 °C for 6 h. This structure-transformation temperature is much higher than the 550 °C needed for the as-synthesized fcc-FePt NPs, as previously reported.^[10,11] Figure 2b is the XRD pattern of the as-synthesized fcc-FePt NPs annealed at 750 °C for 6 h. Comparing Figure 2a and b, we can see that i) the broad diffraction pattern from the FePt/MgO NPs indicates that the FePt in the FePt/MgO structure does not experience grain growth during the high-temperature annealing process; ii) FePt in FePt/MgO adopts a fct-like structure, even though the fully ordered fct structure cannot be confirmed; iii) the diffraction peaks from the FePt/MgO appear at lower angles than the corresponding peaks from the FePt NPs, indicating that the nanostructured FePt in FePt/MgO has a slightly larger crystal-lattice spacing than bulk fct-FePt, which is most likely a result of the imperfect fcc-to-fct transformation and/or FePt NP surface effects; and iv) the fcc-to-fct transition is hindered by the limit of Fe and Pt mobility within the constrained MgO structure.

Magnetic measurements show that the as-synthesized fcc-FePt and fcc-FePt/MgO NPs are superparamagnetic at room temperature. After thermal annealing at 650 °C under Ar + 5% H₂, the uncoated FePt assembly became FM, and the room-temperature coercivity reached 2 T. Under the same annealing conditions, the FePt/MgO NPs show FM properties at low temperatures of 5 K and 100 K, but are superparamagnetic/weakly FM at room temperature, as shown in Figure 3a. Clearly, the annealing at 650 °C for 6 h did not completely convert the fcc-FePt into fct-FePt in the FePt/MgO structure. This is also evidenced from the XRD studies. The fct-FePt/MgO was obtained by annealing the fcc-FePt/MgO at 750 °C for 6 h. Figure 3b shows the hysteresis loops of the fct-FePt/MgO NPs measured at 5 K, 100 K, and 300 K. We can see that these fct-FePt/MgO NPs are

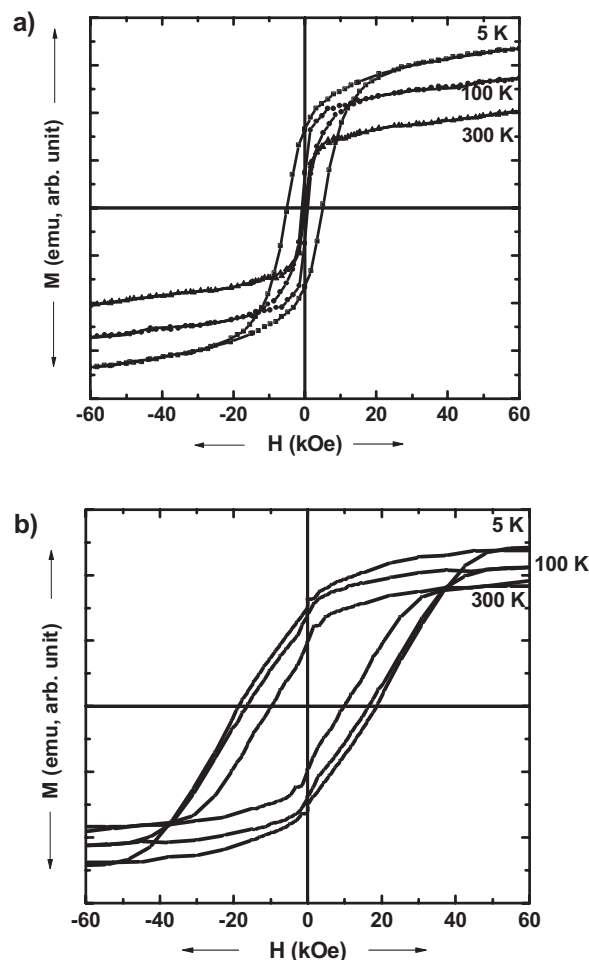


Figure 3. Hysteresis loops of the nanocrystalline FePt/MgO NPs annealed at a) 650 °C, and b) 750 °C for 6 h under Ar + 5% H₂.

FM, with H_c reaching 1.8 T (at 5 K), 1.6 T (at 100 K), and 1 T (at 300 K), respectively. By comparing the structural transformation and magnetic-property change between the uncoated FePt and the coated FePt/MgO, we can conclude that: i) MgO in FePt/MgO protects FePt from sintering at annealing temperatures up to 800 °C; and ii) in a constrained MgO structure, where atom mobility is limited because of the robust MgO coating, the fcc-to-fct conversion is still possible, but is much more difficult, and requires a high annealing temperature (150 °C higher than that for the 7 nm FePt NPs in this work) and longer annealing time.

The fct-FePt/MgO NPs prepared from the thermal annealing of fcc-FePt/MgO NPs are hardly dispersed in any solvent. Although MgO in the FePt/MgO structure can be removed by washing with dilute HCl (0.5 M), the bare fct-FePt NPs quickly aggregate. Adding poly(vinyl pyrrolidone) (PVP) to the aqueous solution during the MgO removal process did not yield any efficient on FePt-NP stabilization. To protect the fct-FePt NPs from aggregation upon MgO removal, we attempted extraction from their aqueous phase into an organic phase by a phase-transfer process. We added the fct-FePt/MgO NPs to a mixture of aqueous 0.5 M HCl and surfactant-containing hexane, to extract the fct-FePt NPs into hexane with their surface protected by the

surfactant. We tested several different surfactant combinations, which included OA/OAm/hexane, HDT/hexane, and HDT/OA/hexane. We found that OA/OAm could not stabilize the fct-FePt NPs under the current extraction conditions. HDT alone offered only temporary stabilization—the NP dispersion became unstable and aggregated after 2 h. The HDT/OA produced the most efficient protection to the fct-FePt NPs. The stabilization difference between HDT and HDT/OA seems to indicate that thiol (SH) reacts with Pt, while COOH binds to Fe, on the surface of the FePt NP, and the double bond in OA is essential for the stabilization, as the saturated hydrocarbon chain tends to fold on the NP surface, which leads to strong NP interactions and aggregation.

Figure 4a outlines the chemistry of transferring the fct-FePt/MgO NPs from their aqueous suspension to the hexane dispersion. In the figure, the bottom layer represents the aqueous solution of 0.5 M HCl for MgO removal, and the upper layer is the hexane phase, with the dispersed fct-FePt NPs coated with HDT/OA. Figure 4b is a photograph that shows the fct-FePt NP hexane dispersion at the top, and the colorless aqueous solution at the bottom, after the FePt extraction by HDT/OA. Figure 4c is a TEM image of the fct-FePt NPs obtained from their hexane dispersion. By comparing with Figure 1a, we can see that there is only a slight morphology change before and after the annealing/MgO removal process. Figure 4d is the high-resolution (HR)TEM image of a single fct-FePt NP, where the (111) lattice fringe is measured to be 0.24 nm, which is larger than the 0.22 nm of the bulk fct-FePt. This is consistent with the lower angle position of the (111) diffraction peak observed in the XRD pattern shown in Figure 2a. Note that after MgO removal,

Fe₄₆Pt₅₄ NPs were obtained, which indicates a small reduction in Fe composition during the acid washing and transfer process. This Fe loss is likely caused by HCl etching. Despite this loss, the fct-FePt NPs obtained from the hexane dispersion are still FM, with a coercivity that reaches near 1 T and magnetization at 56.4 emu per gram of FePt (the data was normalized by weighing the FePt after the removal of the HDT/OA surfactant at 800 °C under argon. As the thiol and the –COOH groups cannot be removed completely from the FePt surface, and the hydrocarbon chain in the surfactant may also form carbon deposits around each NP, the actual magnetization value should be slightly higher.).

In summary, we have reported that a dispersion of FM fct-FePt NPs can be prepared from thermal annealing of the core/shell-structured fcc-FePt/MgO NPs. MgO in FePt/MgO protects the FePt NPs from sintering at high annealing temperatures. In a constrained MgO structure, where atom mobility is limited because of the robust MgO coating, the conversion from fcc- into fct-FePt is possible, but is more difficult compared with the non-MgO-coated FePt NPs, which require a high annealing temperature (150 °C higher). The fct-FePt NPs obtained from the annealing of the fcc-FePt NPs at 750 °C for 6 h show a room-temperature coercivity of 1 T and magnetization of 56.4 emu per gram of FePt. MgO in the fct-FePt/MgO can be removed by acid (HCl) washing, and the fct-FePt NPs are protected by a surfactant combination of hexadecanethiol and oleic acid, which forms a stable hexane dispersion. Such fct-FePt NPs dispersed in hexane should serve as ideal building blocks for constructing FM nanostructures and for information/energy storage applications.

Experimental

Synthesis of 7 nm fcc-Fe₅₁Pt₄₉ NPs: Pt(acac)₂ (0.5 mmol), oleic acid (4 mmol), and oleylamine (4 mmol) were added into a 50 mL four-neck flask that contained 10 mL of octadec-1-ene under gentle argon gas flow. The flask was heated to 120 °C at a heating rate of 6 °C min⁻¹. The flask was maintained for 13 min at this temperature, to ensure the dissolution of Pt(acac)₂. Under a blanket of argon gas, 0.20 mL of Fe(CO)₅ was added. The solution was then heated to 240 °C at a heating rate of 3 °C min⁻¹, and kept at this temperature for 1 h. The heating source was then removed, and the solution was cooled to room temperature, after which the solution was exposed to air. A black product was precipitated by adding 40 mL of ethanol, and separated by centrifugation. The dark-yellow supernatant was discarded. The NPs were dispersed in 15 mL of hexane, and precipitated out by adding 20 mL of ethanol followed by centrifugation. The dispersion/precipitation procedure was repeated three times. Finally, the 7 nm fcc-FePt NPs were re-dispersed in 10 mL of hexane.

Synthesis of fcc-Fe₅₁Pt₄₉/MgO NPs: Mg(acac)₂ (2 mmol), tetradecane-1,2-diol (4 mmol), oleic acid (4 mmol), and oleylamine (4 mmol) were mixed with 20 mL of benzyl ether and heated to 80 °C. The 7 nm FePt NPs (~100 mg) dispersed in 5 mL of hexane were rapidly added into the reaction solution, within ~2 s. The solution was heated to 120 °C to remove hexane. Under nitrogen gas, the solution was heated to reflux (298 °C), and kept at this temperature for 1 h. The fcc-FePt/MgO NPs were separated and purified by using hexane, ethanol, and centrifugation. Finally, the particles were kept in 5 mL hexane.

Characterization: The size, morphology, and structure of the FePt NPs were characterized using a Philips EM 420 (120 kV) and a JEOL 2010 (200 kV). X-ray powder diffraction patterns were recorded using a Bruker AXS D8-Advanced diffractometer with Cu K α radiation ($\lambda = 1.5418 \text{ \AA}$). Magnetic studies were performed using a Quantum Design Superconducting Quantum Interface Device (SQUID) with a field up to 70 kOe.

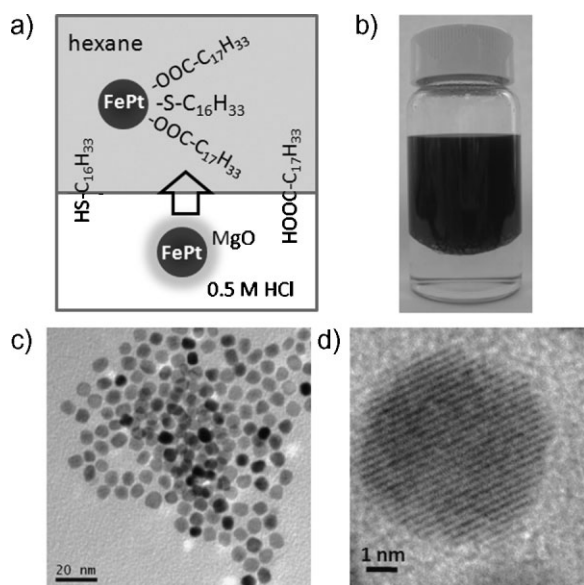


Figure 4. a) Schematic illustration of the fct-FePt NP transfer from the 0.5 M HCl aqueous phase to the hexane phase. b) Photograph showing the fct-FePt NP transfer from the aqueous phase to the hexane phase (the fct-FePt NPs are obtained from the FePt/MgO NPs with magnetic properties, shown in Figure 3b). c) TEM image of the fct-FePt NPs from b). d) HRTEM image of a single fct-FePt NP with interfringe spacing at 0.24 nm.

NP compositions were analyzed by Oxford energy-disperse X-ray spectroscopy and inductively coupled plasma–atomic emission spectroscopy.

Acknowledgements

The work was supported by ONR/MURI under grant Nos N00014–05–1–0497.

Received: June 13, 2008

Revised: August 14, 2008

Published online: December 18, 2008

-
- [1] S. Sun, *Adv. Mater.* **2006**, *18*, 393.
 [2] D. Weller, M. F. Doerner, *Annu. Rev. Mater. Sci.* **2000**, *30*, 611.
 [3] A. Moser, K. Takano, D. T. Margulies, M. Albrecht, Y. Sonobe, Y. Ikeda, S. Sun, E. E. Fullerton, *J. Phys. D: Appl. Phys.* **2002**, *35*, R157.
 [4] I. R. McFadyen, E. E. Fullerton, M. J. Carey, *MRS Bull.* **2006**, *31*, 379.
 [5] E. F. Kneller, R. Hawig, *IEEE Trans. Magn.* **1991**, *27*, 3588.
 [6] R. Skomski, J. M. D. Coey, *Phys. Rev. B* **1993**, *48*, 15812.
 [7] T. Schrefl, H. Kronmüller, J. Fidler, *J. Magn. Mag. Mater.* **1993**, *127*, L273.
 [8] H. Zeng, J. Li, J. P. Liu, Z. L. Wang, S. Sun, *Nature* **2002**, *420*, 395.
 [9] S. D. Bader, *Rev. Mod. Phys.* **2006**, *78*, 1.
 [10] S. Sun, C. B. Murray, D. Weller, L. Folks, A. Moser, *Science* **2000**, *287*, 1989.
 [11] S. Sun, E. E. Fullerton, D. Weller, C. B. Murray, *IEEE Trans. Magn.* **2001**, *37*, 1239.
 [12] M. Chen, J. P. Liu, S. Sun, *J. Am. Chem. Soc.* **2004**, *126*, 8394.
 [13] S. Momose, H. Kodama, T. Uzumaki, A. Tanaka, *Jpn. J. Appl. Phys.* **2005**, *44*, 1147.
 [14] S. Sun, S. Anders, T. Thomson, J. E. E. Baglin, M. F. Toney, H. F. Hamann, C. B. Murray, B. D. Terris, *J. Phys. Chem. B* **2003**, *107*, 5419.
 [15] K. E. Elkins, T. S. Vedantam, J. P. Liu, H. Zeng, S. Sun, Z. L. Wang, Y. Ding, *Nano Lett.* **2003**, *3*, 1647.
 [16] C. Liu, X. Wu, T. Klemmer, N. Shukla, X. Yang, D. Weller, A. G. Roy, M. Tanase, D. Laughlin, *J. Phys. Chem. B* **2004**, *108*, 6121.
 [17] B. Jeyadevan, A. Hobo, K. Urakawa, C. N. Chinnasamy, K. Shinoda, K. Tohji, *J. Appl. Phys.* **2003**, *93*, 7574.
 [18] T. Iwaki, Y. Kakihara, T. Toda, M. Abdullah, K. Okuyama, *J. Appl. Phys.* **2003**, *94*, 6807.
 [19] Y. Kitamoto, R. Minami, Y. Shibata, T. Chikata, S. Kato, *IEEE Trans. Magn.* **2005**, *41*, 3880.
 [20] S. Yamamoto, Y. Morimoto, T. Ono, M. Takano, *Appl. Phys. Lett.* **2005**, *87*, 032503.
 [21] S. Yamamoto, Y. Morimoto, Y. Tamada, Y. K. Takahashi, K. Hono, T. Ono, M. Takano, *Chem. Mater.* **2006**, *18*, 5385.
 [22] Y. Tamada, Y. Morimoto, S. Yamamoto, M. Takano, S. Nasu, T. Ono, *J. Magn. Magn. Mater.* **2007**, *310*, 2381.
 [23] Y. Tamada, S. Yamamoto, M. Takano, S. Nasu, T. Ono, *Appl. Phys. Lett.* **2007**, *90*, 162 509.
 [24] K. Elkins, D. Li, N. Poudyal, V. Nandwana, Z. Jin, K. Chen, J. P. Liu, *J. Phys. D: Appl. Phys.* **2005**, *38*, 2306.
 [25] D. R. Li, N. Poudyal, V. Nandwana, Z. Q. Jin, K. Elkins, J. P. Liu, *J. Appl. Phys.* **2006**, *99*, 08E 911.
 [26] B. A. Jones, J. D. Dutson, K. O'Grady, B. J. Hickey, D. R. Li, N. Poudyal, J. P. Liu, *IEEE Trans. Magn.* **2006**, *42*, 3066.
 [27] C. B. Rong, N. Poudyal, G. S. Chaubey, V. Nandwana, Y. Liu, Y. Q. Wu, M. J. Kramer, M. E. Kozlov, R. H. Baughman, J. P. Liu, *J. Appl. Phys.* **2008**, *103*, 07E 131.
 [28] D. Zanchet, M. S. Moreno, D. Ugarte, *Phys. Rev. Lett.* **1999**, *82*, 5277.
-